



# Geophysical Research Letters

## RESEARCH LETTER

10.1029/2019GL085498

### Key Points:

- Observations show atypical radical precursors drive >70% of atmospheric oxidation in polluted air over the northeast United States during winter
- Anthropogenic emissions and multiphase chemistry largely control the abundance of these atypical radical precursors
- Improved descriptions of these radical sources in air quality models are needed to predict future trajectories in wintertime air pollution

### Supporting Information:

- Supporting Information S1

### Correspondence to:

J. A. Thornton,  
thornton@atmos.washington.edu

### Citation:

Haskins, J. D., Lopez-Hilfiker, F. D., Lee, B. H., Shah, V., Wolfe, G. M., DiGangi, J., et al. (2019).

Anthropogenic control over wintertime oxidation of atmospheric pollutants.

*Geophysical Research Letters*, 46, 14,826–14,835. <https://doi.org/10.1029/2019GL085498>

Received 23 SEP 2019

Accepted 11 DEC 2019

Accepted article online 13 DEC 2019

Published online 20 DEC 2019

## Anthropogenic Control Over Wintertime Oxidation of Atmospheric Pollutants

J. D. Haskins<sup>1</sup>, F. D. Lopez-Hilfiker<sup>1,2</sup>, B. H. Lee<sup>1</sup>, V. Shah<sup>1,3</sup>, G. M. Wolfe<sup>4,5</sup>, J. DiGangi<sup>6</sup>, D. Fibiger<sup>7,8,9</sup>, E. E. McDuffie<sup>7,8,10,11</sup>, P. Veres<sup>7</sup>, J. C. Schroder<sup>7,10</sup>, P. Campuzano-Jost<sup>7,10</sup>, D. A. Day<sup>7,10</sup>, J. L. Jimenez<sup>7,10</sup>, A. Weinheimer<sup>12</sup>, T. Sparks<sup>13</sup>, R. C. Cohen<sup>13</sup>, T. Campos<sup>12</sup>, A. Sullivan<sup>14</sup>, H. Guo<sup>15</sup>, R. Weber<sup>15</sup>, J. Dibb<sup>16</sup>, J. Green<sup>17</sup>, M. Fiddler<sup>17</sup>, S. Bililign<sup>17</sup>, L. Jaeglé<sup>1</sup>, S. S. Brown<sup>8,10</sup>, and J. A. Thornton<sup>1</sup>

<sup>1</sup>Department of Atmospheric Sciences, University of Washington, Seattle, WA, USA, <sup>2</sup>Now at Tofwerk AG, Thun, Switzerland, <sup>3</sup>Now at Harvard John A. Paulson School of Engineering and Applied Sciences, Harvard University, Cambridge, MA, USA, <sup>4</sup>Joint Center for Earth Systems Technology, University of Maryland, Baltimore County, Baltimore, MD, USA, <sup>5</sup>Atmospheric Chemistry and Dynamics Laboratory, NASA Goddard Space Flight Center, Greenbelt, MD, USA, <sup>6</sup>NASA Langley Research Center, Hampton, VA, USA, <sup>7</sup>Cooperative Institute for Research in Environmental Sciences, University of Colorado Boulder, Boulder, CO, USA, <sup>8</sup>Chemical Sciences Division, NOAA Earth System Research Laboratory, Boulder, CO, USA, <sup>9</sup>Now at California Air Resources Board, Sacramento, CA, USA, <sup>10</sup>Department of Chemistry, University of Colorado Boulder, Boulder, CO, USA, <sup>11</sup>Now at the Department of Physics and Atmospheric Science, Dalhousie University, Halifax, Nova Scotia, Canada, <sup>12</sup>Earth Observing Laboratory, National Center for Atmospheric Research, Boulder, CO, USA, <sup>13</sup>Department of Chemistry, University of California, Berkeley, CA, USA, <sup>14</sup>Department of Atmospheric Sciences, Colorado State University, Fort Collins, CO, USA, <sup>15</sup>School of Earth and Atmospheric Sciences, Georgia Institute of Technology, Atlanta, GA, USA, <sup>16</sup>Department of Earth Sciences, University of New Hampshire, Durham, NH, USA, <sup>17</sup>Department of Physics, North Carolina Agricultural and Technical State University, Greensboro, NC, USA

**Abstract** During winter in the midlatitudes, photochemical oxidation is significantly slower than in summer and the main radical oxidants driving formation of secondary pollutants, such as fine particulate matter and ozone, remain uncertain, owing to a lack of observations in this season. Using airborne observations, we quantify the contribution of various oxidants on a regional basis during winter, enabling improved chemical descriptions of wintertime air pollution transformations. We show that 25–60% of NO<sub>x</sub> is converted to N<sub>2</sub>O<sub>5</sub> via multiphase reactions between gas-phase nitrogen oxide reservoirs and aerosol particles, with ~93% reacting in the marine boundary layer to form >2.5 ppbv ClNO<sub>2</sub>. This results in >70% of the oxidizing capacity of polluted air during winter being controlled by multiphase reactions and emissions of volatile organic compounds, such as HCHO, rather than reaction with OH. These findings highlight the control local anthropogenic emissions have on the oxidizing capacity of the polluted wintertime atmosphere.

**Plain Language Summary** During summer, rapid transformations of primary pollutants, those emitted directly into the atmosphere, into secondary pollutants, such as particulate matter and ozone, are driven by reactions with the hydroxyl radical, formed in the atmosphere when sunlight strikes ozone in the presence of water vapor. During winter, when there is less sunlight and water vapor, production of this radical is lower. Yet the conversion of primary pollutants into secondary pollutants still occurs rapidly, pointing to a misunderstanding in the chemical processes that drive this conversion during winter. Using aircraft data collected across the northeast United States during the winter of 2015, we show that reactions with radicals arising from atypical precursors, such as nitryl chloride, account for more than 70% of the reactions that directly emitted pollutants undergo. We show that during winter, the formation of these radicals is tied to human activities. Our data provide critical constraints for improving the descriptions of chemical processes in air quality models, which will help guide improved air quality policy. Other regions of the world, such as China, Europe, and northern India, also experience this seasonal chemical shift in the atmosphere. Our findings, therefore, have global scale implications for understanding wintertime pollution transformations and transport.

## 1. Introduction

Atmospheric primary radicals, formed from the photolysis of closed-shell molecules, initiate and sustain oxidation cycles during air pollution episodes. Understanding the sources of these radicals is a key scientific challenge for designing pollution mitigation strategies because they drive conversion of primary pollutants into secondary pollutants such as ozone (O<sub>3</sub>) and fine particulate matter (PM<sub>2.5</sub>). In summer, production of hydroxyl radicals (OH) through O<sub>3</sub> photolysis is often the dominant daily integrated primary radical source due to high water vapor, O<sub>3</sub>, and solar radiation.



Other smaller summertime sources of hydrogen oxide radicals (HO<sub>x</sub> = OH + HO<sub>2</sub>) can include formaldehyde (HCHO) and nitrous acid (HONO) photolysis (Michoud et al., 2012; Volkamer et al., 2010; Whalley et al., 2018; Young et al., 2014).

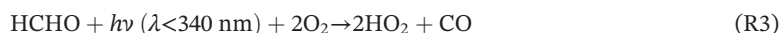
During winter, (R1) is slower by more than an order of magnitude due to reduced sunlight and reduced water vapor (Yienger et al., 1999), suggesting greater importance of other less well quantified radical sources. Moreover, colder temperatures and less photochemical oxidation increase the importance of multiphase interactions, between trace gases, particulate matter, and cloud and fog droplets, in driving the chemical evolution of primary pollutants. The sources of atypical radical precursors that might drive photochemical oxidation, multiphase chemical processing, and the interplay between these processes remain highly uncertain and indubitably cause some of the problems air quality models have in describing wintertime air pollution (Edwards et al., 2014; Gao et al., 2016; Heald et al., 2012).

HONO photolysis (R2) can be an important OH radical source at low light levels typical of winter (Kleffmann, 2007; VandenBoer et al., 2013; Wong et al., 2012).



HONO is directly emitted from combustion (Kirchstetter et al., 1996) and formed in situ from the heterogeneous uptake of NO<sub>2</sub> on surfaces (Stutz et al., 2002; Kleffmann et al., 2007). Daytime HONO concentrations in excess of that expected from these sources are routinely observed (Sorgel et al., 2011; VandenBoer et al., 2013; Wong et al., 2012), leading to numerous in situ multiphase production mechanisms being proposed (Spataro & Ianniello, 2014). However, there is not yet consensus on the abundance, production mechanisms, and seasonality of daytime HONO.

Photochemical oxidation of hydrocarbons in the presence of nitrogen oxide radicals (NO<sub>x</sub> = NO + NO<sub>2</sub>) can amplify the primary radical sources by leading to photolabile intermediates such as HCHO (Levy, 1971):

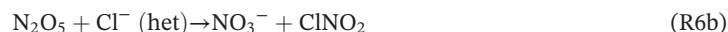


In the lowest kilometer of the atmosphere, oxidation of the biogenic hydrocarbon, isoprene, is typically the largest regional source of HCHO during summer (Wolfe, Kaiser, et al., 2016). During winter, negligible biogenic isoprene emissions and lower radical concentrations are expected to reduce the production and abundance of HCHO. Thus, the importance of HCHO as a radical source in winter will depend upon direct emissions of HCHO and potential precursors from inefficient combustion, manufacturing processes, and consumer products, all of which remain poorly constrained (Altshuller, 1993; Anderson et al., 1996; Kelly et al., 1999; McDonald et al., 2018; Sigsby et al., 1987).

Coincident with seasonal shifts in photochemistry, multiphase chemical processes that occur in aerosol particles and clouds are promoted in winter relative to summer (Shah et al., 2018). A prime example is dinitrogen pentoxide (N<sub>2</sub>O<sub>5</sub>), formed from the reaction of NO<sub>2</sub> with O<sub>3</sub> to generate the nitrate radical (NO<sub>3</sub>), which, subsequently reacts with another NO<sub>2</sub> molecule, (Platt et al., 1984). N<sub>2</sub>O<sub>5</sub> hydrolysis on aqueous particles (R6a) is a major sink of NO<sub>x</sub> during winter, which in turn limits daytime radical cycling (Dentener & Crutzen, 1993).

When particles contain chloride, N<sub>2</sub>O<sub>5</sub> reactions can also form ClNO<sub>2</sub> (Behnke et al., 1997; Finlayson-Pitts et al., 1989), which undergoes photolysis via (R7) during the early morning, releasing NO<sub>x</sub> and highly

reactive chlorine atoms (Cl). Cl atoms initiate the oxidation of various hydrocarbons (RH), in some cases up to 100 times faster than OH, (R8) (Orlando et al., 2003).



Resolving whether the multiphase chemistry of  $\text{N}_2\text{O}_5$  is a net sink of radical precursors via, or source of radical precursors (R6b) during winter is a key challenge.

In this work, we utilize recent observations from the Wintertime Investigation of Transport, Emissions, and Reactivity (WINTER) campaign to assess the wintertime primary radical sources in polluted regions of the eastern United States. We find that in polluted air, the regional daily integrated primary radical source is dominated by  $\text{ClNO}_2$ ,  $\text{HCHO}$ , and to a lesser extent HONO.

## 2. Methods

The National Science Foundation/National Center for Atmospheric Research C-130 aircraft was utilized during the WINTER campaign to make airborne observations of many of the above radical precursors as well as related primary and secondary pollutants from 1 February to 15 March 2015. More details on the WINTER campaign instrumentation and results can be found in the supporting information (SI) as well as the WINTER special issue of the Journal of Geophysical Research. Thirteen research flights (Figure S1) were conducted over the eastern United States, with ~50% of flight hours occurring at night, and more than 80% within 1 km of the surface.

## 3. Results and Analysis

Using the suite of in situ observations made during WINTER, we can assess the contribution of each radical source discussed above to the oxidative capacity of the wintertime troposphere. For example, observations of all components involved in the conversion of  $\text{NO}_x$  to  $\text{N}_2\text{O}_5$  and its multiphase reaction products (Figure 1) were made during a flight downwind of New York City, when westerly winds exported urban  $\text{NO}_x$  emissions into the marine boundary layer (MBL) over the Atlantic Ocean. Mixing ratios of  $\text{ClNO}_2$ ,  $\text{N}_2\text{O}_5$ ,  $\text{HNO}_3$ , and HONO measured by mass spectrometry, together with NO and  $\text{NO}_2$  measured by chemiluminescence and cavity ring-down spectroscopy (Figure 1, top panels) explain the independently measured sum total of reactive nitrogen oxides ( $\text{NO}_y = \text{NO}_x + 2 * \text{N}_2\text{O}_5 + \text{ClNO}_2 + \text{HNO}_3 + \text{HONO} + \text{alkyl nitrates} + \text{peroxy acetyl nitrates, PANs}$ ) at all points along this flight (Figure 1, bottom). Our observations show that ~25–60% of  $\text{NO}_x$  is converted to  $\text{N}_2\text{O}_5$  on this flight, with ~93% reacting in the MBL to form  $\text{HNO}_3$  and  $\text{ClNO}_2$  (Jaeglé et al., 2018), highlighting the importance of multiphase chemistry under such conditions.

We use the observed nighttime concentrations of  $\text{O}_3$ ,  $\text{ClNO}_2$ ,  $\text{HCHO}$ , and HONO together with average WINTER measured photolysis frequencies to calculate the total integrated concentration of radicals that would be produced by these precursors over the following day (see SI section S3b). Other radical sources, such as alkene ozonolysis or dihalogen ( $\text{Cl}_2$ ) photolysis (Haskins et al., 2018), were <5% on a regional basis during WINTER (see SI Figure S6 and Figure 2). While the nocturnal surface layer is poorly mixed over land, vertical profiling performed by the aircraft allowed us to assess the vertical extent of these radical precursors. We found the MBL to be well mixed up to 800- to 1,500-m altitude (e.g., Figure 2), allowing more straightforward calculations of radical sources from measured concentrations.

During the flight shown in Figure 1,  $\text{ClNO}_2$  becomes the largest measured radical reservoir, contributing at least 38% to the calculated next-day integrated radical source, with similar contributions from  $\text{HCHO}$  and  $\text{O}_3$

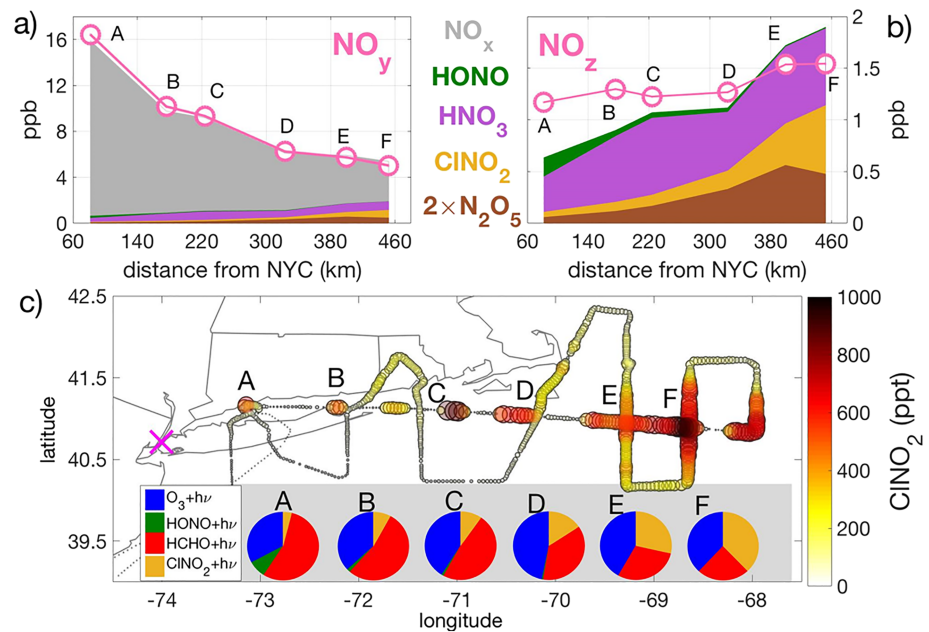


**Figure 1.** Evolution of nitrogen oxide reservoir species downwind of New York City (purple x) observed during Research Flight 3 of the WINTER campaign. (a) NO<sub>y</sub> is the sum of all forms of reactive nitrogen oxides that can be converted to NO at high temperatures. (b) NO<sub>z</sub> is the sum of higher oxides of all reactive nitrogen oxides species excluding NO<sub>x</sub> (NO<sub>z</sub> = NO<sub>y</sub> - NO<sub>x</sub>). The gap between NO<sub>z</sub> and the sum of the individual components that occurs near NYC is likely explained by a combination of particle nitrates and gaseous peroxy nitrates (see Supporting Information). (c) Map of the flight track colored and sized by the measured mixing ratio of ClNO<sub>2</sub>. The pie charts show the observationally constrained contributions of different radical precursors to the integrated daytime radical source (see text). The six intercepts of the New York City plume, labeled as A–F in (a)–(c), occurred between 7 p.m. to 11 p.m. local time, between 250- and 400-m pressure altitudes (c). The Plume Intercept F was excluded due to a higher altitude (750 m) than the first six.

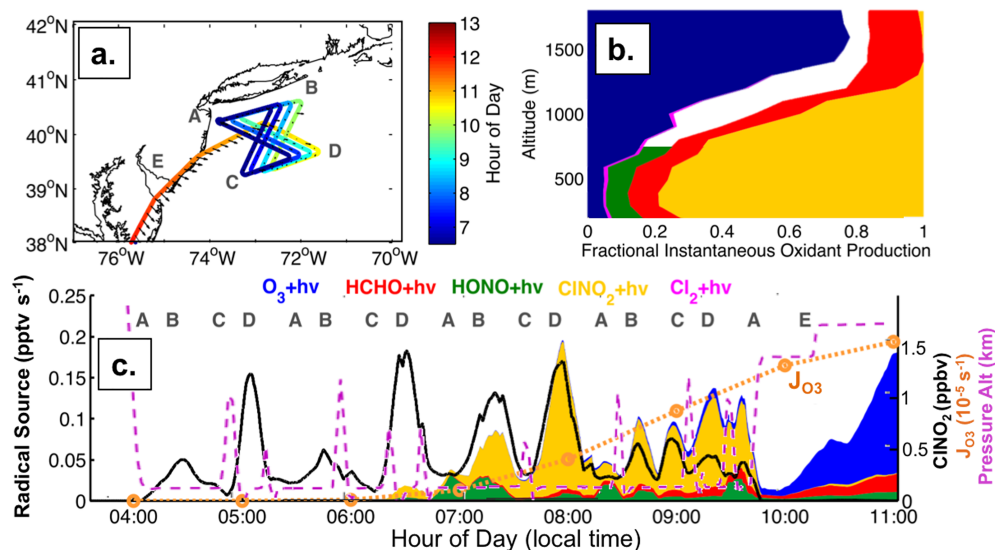


**Figure 2.** (a) Flight track of the NSF/NCAR C-130 on Research Flight 8 of the WINTER campaign, colored by local time of day. Sunrise occurred at approximately 6:30 a.m. local time. Only portions with altitudes <2,000 m are shown. (b) Vertical profiles of the instantaneous radical source calculated from observations of solar radiation and radical precursors. White space indicates HONO measurements at these altitudes were below instrument detection limits. (c) Time series of the instantaneous radical source (left axis, stacked color), ClNO<sub>2</sub> mixing ratios (right axis, ppbv), the measured O<sub>3</sub> photolysis frequency (orange circles, right axis, 10<sup>-5</sup> s<sup>-1</sup>), and pressure altitude (right axis, km)



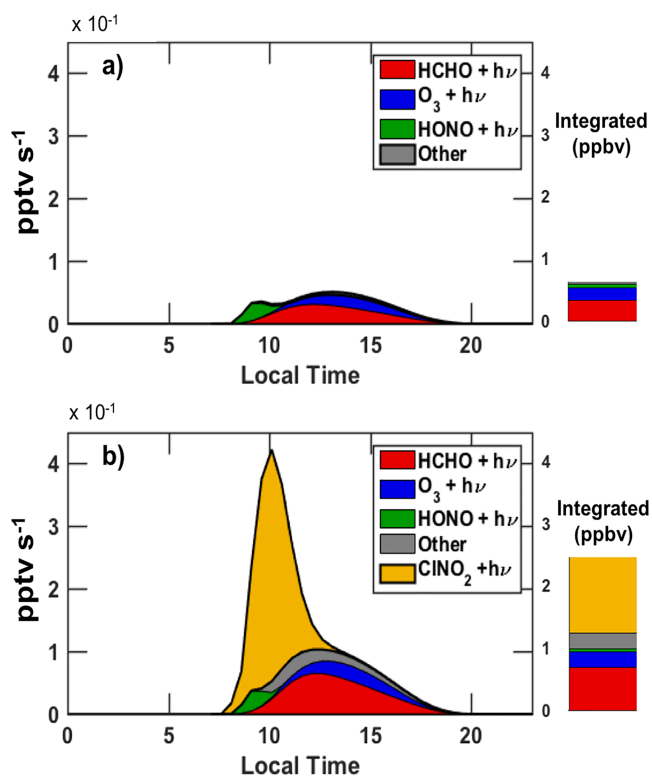


**Figure 3.** Summary of daily integrated primary radical production rates calculated the day following our interception of the peak  $\text{ClNO}_2$  concentrations on RF08 using the FOAM box model initialized with WINTER observations without including chlorine reactions (a) and including chlorine reactions (b). Bar charts show the integrated daily radical source from each precursor.

chemistry which removes  $\text{O}_3$  ((R2)–(R4)) (Brown et al., 2006). The aircraft departed the area (Segment E, Figure 2a) flying above the MBL where we find that the radical source is dominated by that from  $\text{O}_3$  photolysis (R1), as expected, given the steep gradients in  $\text{ClNO}_2$  between the polluted boundary layer and free troposphere.

To further evaluate the implications of these results, we use a chemically explicit Master Chemical Mechanism based 0-D model (FOAM, Wolfe, Marvin et al., 2016) to simulate radical chemistry during the full day following the interception of these plumes. We perform two simulations, including and excluding reactions of Cl atoms with various volatile organic compounds (VOCs; ((R8)b–R10), using the mechanism described in Riedel et al. (2014) (see SI section S4). The model is initialized with WINTER measurements of VOCs and other gas-phase species including HCHO, HONO,  $\text{O}_3$ ,  $\text{N}_2\text{O}_5$ , and  $\text{ClNO}_2$  (see Supporting Information for details). Figure 3 shows the modeled instantaneous radical production occurring for 16 hr following our interception of the maximum  $\text{ClNO}_2$  concentration (6:36 a.m., Location “D,” Figure 2). We also initialized the model with median  $\text{ClNO}_2$  concentration from all intercepts in this flight, results are briefly discussed below and shown in the Supporting Information.

Consistent with our above observational analysis, the model predicts an instantaneous radical production rate from  $\text{ClNO}_2$  that is a factor of 5–12 larger than the next largest radical source between 6 a.m. and 11 a.m. (Figure 3).  $\text{ClNO}_2$  also dominates the total daily integrated radical source predicted with the model. The simulation including chlorine chemistry produced 2.5 ppbv of radicals ( $\text{Cl} + \text{HO}_x + \text{RO}_2$ ) by day’s end, which is a factor of 3.75 larger than that predicted without chlorine chemistry. The increase in radical production stems from Cl radicals from  $\text{ClNO}_2$  photolysis, a secondary 114% enhancement (0.62 ppbv) in HCHO due to Cl radical initiated VOC oxidation (see SI section S4) and an increase in ozone production. Using median  $\text{ClNO}_2$  concentrations similarly led to the total radical source being a factor of 3.1 larger than when neglecting Cl radical chemistry. The magnitude of the  $\text{HO}_x$  enhancement could be different for

((R1) and (R3)) but negligible contributions from HONO. This integrated radical source calculation is based upon measurements made before local midnight, and several more hours of  $\text{ClNO}_2$  production could be expected. Assuming  $\text{N}_2\text{O}_5$  formation continued as observed  $\text{NO}_2$  and  $\text{O}_3$  would suggest and an  $\text{N}_2\text{O}_5$  reactivity on aerosols from in situ observations (McDuffie et al., 2018; McDuffie et al., 2018), we estimate  $\text{ClNO}_2$  concentrations would increase throughout the night and account for as much as 80% ( $[\text{ClNO}_2] \sim 1,500$  pptv) of the integrated radical source the next day. This result, assuming no further changes to  $\text{O}_3$ , HCHO, or HONO, highlights the important role of anthropogenic  $\text{NO}_x$  emissions in wintertime radical sources. Estimates of  $\text{ClNO}_2$  contributions to the summertime radical budget have been substantially less (8–20%) (Young et al., 2014).

During a second WINTER flight, a stalled high-pressure system offshore of New Jersey (Figure 2a) allowed us to probe the instantaneous morning radical source (see SI) in pollution from the New York City area that had aged overnight in the MBL. As the Sun rose, vertical profiles (Figure 2b) with the aircraft revealed that the observed instantaneous radical source from  $\text{ClNO}_2$  photolysis,  $j_{\text{ClNO}_2}(t) * [\text{ClNO}_2(t)]$ , was 60–80% of the total instantaneous radical source throughout the entire MBL (SI section S3a).

During this flight, HONO photolysis was the next largest instantaneous radical source. Contributions from  $\text{Cl}_2$  were low, given small (<15 pptv) observed concentrations (Haskins et al., 2018).  $\text{ClNO}_2$  reactive uptake to form  $\text{Cl}_2$ , which would amplify the radical source stemming from  $\text{N}_2\text{O}_5$  chemistry, was also small (Haskins et al., 2019). R1 was negligible in the flight shown in Figure 2.  $\text{O}_3$  mixing ratios are often suppressed in  $\text{NO}_x$ -rich air masses during the night and morning, in part due to nighttime  $\text{N}_2\text{O}_5$

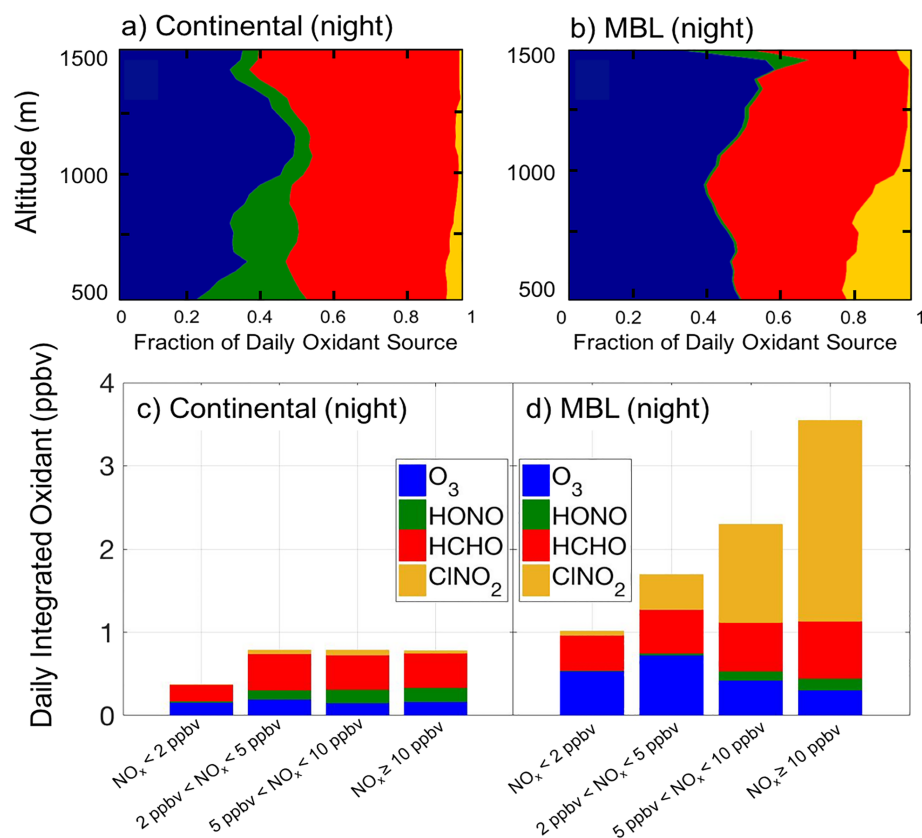


**Figure 4.** Vertical profiles of the daily integrated primary radical sources calculated from observations of O<sub>3</sub>, H<sub>2</sub>O, ClNO<sub>2</sub>, HONO, and HCHO made throughout the campaign in vertical profiling maneuvers during the night below 1.5 km over (a) the continental boundary layer and (b) within the marine boundary layer (MBL). Averaging over these vertical profiles during the night and binning them as a function of their observed NO<sub>x</sub> mixing ratios, we show the calculated the daily integrated primary radical source from each radical precursor that would result the following day over (c) the continental boundary layer and (d) within the MBL as calculated using the methodology in section S3b of the SI.

different locations and time periods, especially with a different mix of VOC, but these results underscore that including Cl-atom chemistry from ClNO<sub>2</sub> is necessary to represent wintertime oxidation, given the secondary impacts of Cl atoms on HCHO and O<sub>3</sub>.

We apply the above daily integrated radical source analysis to the wider set of flights (see SI section S3b) using predicted photolysis rates and observations of the radical precursors made at night and early morning within 1 km of the surface. Daytime observations underestimate the overall contributions of HONO and ClNO<sub>2</sub> to the total primary radical source because both species photolyze rapidly and may not be reformed until night. The results, shown in Figure 4, illustrate that >70% of the wintertime radical source in polluted air (represented by increasing NO<sub>x</sub>) stems not from reaction (R1) as it would in summer, but from ClNO<sub>2</sub>, HCHO, and HONO photolysis. ClNO<sub>2</sub> and HCHO tend to dominate, but with a strong spatial (vertical and horizontal) dependence reflecting distribution of emission sources, relative lifetimes, and mixing.

The control of local and regional anthropogenic emissions on primary radical sources during winter is evident when considering the contributions of HCHO. HCHO contributes most to the observed radical budget outside of the MBL (Figures 1 and 4). Jaeglé et al. (2018) showed that the standard GEOS-Chem model underestimated observed HCHO during WINTER by a factor of 2, but increasing anthropogenic emissions of HCHO from 10% to 30% of the total HCHO source brought the model into agreement. Increasing emissions of short-lived anthropogenic HCHO precursors, such as ethene and other primary alkenes, followed by their oxidation to form HCHO would also be consistent with the WINTER observations. The extent to which measured alkenes explain the HCHO should be evaluated. Ultimately, the resulting modeled wintertime HCHO

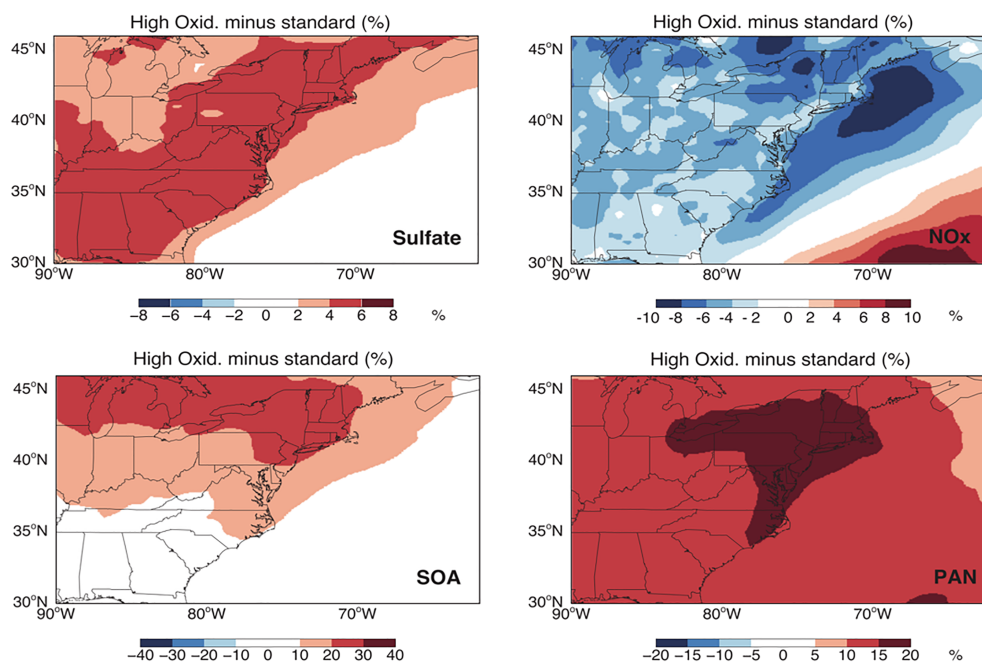


**Figure 5.** Relative changes in GEOS-Chem model predicted particulate sulfate, SOA, NO<sub>x</sub>, and PAN abundances between runs using standard emissions and chemistry, and those using updated emissions of HCHO and updated CINO<sub>2</sub> chemistry (described in Jaeglé et al., 2018) based on the WINTER observations. Enhanced oxidative capacity in the boundary layer from enhanced HCHO (over land) and CINO<sub>2</sub> (in the MBL) leads to increased conversion of SO<sub>2</sub> to sulfate aerosol mass, VOC to secondary organic aerosol mass, and increased conversion of NO<sub>x</sub> into reservoirs such as PAN, which in turn affects its global distribution.

is primarily from anthropogenic sources, in stark contrast to summer. Although smaller than the isoprene dominated source in summertime (Fortems-Cheiney et al., 2012; Luecken et al., 2012; Wolfe et al., 2016), the total HCHO source we estimate during WINTER demonstrates the seasonally varying sensitivity of the radical budget to both anthropogenic and biogenic VOC emissions.

The measured nighttime HONO concentrations during WINTER imply it is a small but nonnegligible contributor to the primary daytime radical source, especially in urban areas close to the surface (<100 m, see SI section S6), but not in the MBL. For example, HONO contributed a maximum of 8% to the projected daily radical budget on the flight shown in Figure 1, but over land HONO contributed 10–20% to the radical budget at the lowest altitudes surveyed, consistent with its main sources being tied to anthropogenic emissions. Somewhat surprisingly, our observations suggest a smaller role for HONO on a regional basis in the daily integrated radical budget than might be inferred from ground-based observations (Whalley et al., 2018). Near-source measurements in a poorly mixed nocturnal atmosphere may tend to overestimate the regional impact of this source (Febo et al., 1996; Stutz et al., 2002; Wong et al., 2012).

Recent studies suggest particulate nitrate ( $\text{pNO}_3^-$ ) photolysis may be an important daytime HONO source, but the rate remains debated (Romer et al., 2018; Ye et al., 2016). We use early morning observations of HONO to predict the production of radicals resulting from its photolysis, assuming no daytime production or further emission of HONO in the analysis presented in Figure 4. Therefore, we would underpredict the contribution from HONO to the primary radical sources if photolysis of  $\text{pNO}_3^-$  or other daytime HONO sources are significant. Our simultaneous observations of  $\text{pNO}_3^-$  and HONO suggest a slow daytime production of HONO from  $\text{pNO}_3^-$  photolysis, similar to the rate presented in Romer et al. (2018), which would increase the total radical source shown in Figure 4 by ~4% over land, with smaller contributions in the polluted MBL (SI Figure S7). Daytime HONO concentrations were often at or below our detection limit (30 pptv); thus, we can only constrain an upper limit source of daytime HONO (see SI section S6).

HCHO emissions, the multiphase chemistry of NO<sub>x</sub>, and aerosol processes that produce and directly affect CINO<sub>2</sub>,  $\text{pNO}_3^-$ , and HONO concentrations, are highly parameterized components of air quality and chemistry-climate models, if included at all (Evans & Jacob, 2005; Riemer et al., 2003; Bertram &

Thornton, 2009). Increasing anthropogenic HCHO sources (Jaeglé et al., 2018) and implementing the production of ClNO<sub>2</sub> (Shah et al., 2018) in the GEOS-Chem model, we find significant impacts on primary and secondary pollutant abundance and air quality metrics relative to the standard model run. For example, PM<sub>2.5</sub> components, such as secondary organic aerosol and sulfate increase by 0.3 μg/m<sup>3</sup> (20–30%) and 0.12 μg/m<sup>3</sup> (2–6%), respectively, while nitrate decreases by up to 0.25 μg/m<sup>3</sup> (0–5%) (Jaeglé et al., 2018), and NO<sub>x</sub> shifts further into its labile reservoirs, such as PAN (see Figure 5). Given PAN's longer lifetime in winter, this transports NO<sub>x</sub> further downwind than during summer. These changes are driven by 40–80% increases in HO<sub>x</sub> and RO<sub>2</sub> radical concentrations across the WINTER domain from increased HCHO photolysis and VOC + Cl reactions, with concomitant increases in ozone production.

Wintertime sulfate is often underestimated by air quality models, while pNO<sub>3</sub><sup>−</sup> and nitrate deposition over land have been overestimated (Gao et al., 2016; Heald et al., 2012; Tesche et al., 2006; Walker et al., 2012). The increases in regional radical sources and changes to NO<sub>x</sub> multiphase chemistry we suggest reduce such discrepancies (Jaeglé et al., 2018; Shah et al., 2018) and also halve GEOS-Chem underestimates (from 30% to 15% bias) of measured total peroxy nitrates (such as PAN). Recent results show that while models of the WINTER domain predict organic aerosol from primary sources, most organic aerosol sampled is formed secondarily in processes like those that occur during summer (Schroder et al., 2018; Sullivan et al., 2019). Ultimately, our results provide support for increased oxidation initiated by atypical radical precursors, and increased export of NO<sub>x</sub> reservoirs to the global free troposphere.

#### 4. Conclusions

We have shown that anthropogenic emissions of NO<sub>x</sub>, and HCHO and its precursors, exert control over radical sources in polluted air during winter. We provide novel and unique observational confirmation that conversion of NO<sub>2</sub> to ClNO<sub>2</sub> represents a critically important wintertime radical source throughout the polluted MBL. In polluted maritime regions, we find that Cl atoms from direct ClNO<sub>2</sub> photolysis are both the dominant early morning radical source and the dominant integrated daily radical source and that their presence amplifies the OH source by increasing HCHO formation from VOC + Cl reactions and increased O<sub>3</sub> production. HCHO is the largest radical source on a regional basis over land, and the dormant wintertime biosphere implies the HCHO sources are dominated by local or regional anthropogenic contributions, either through direct emissions and/or emissions of short-lived precursors, such as primary alkenes.

As the HCHO source evaluation implies, it is possible some reactive VOC, such as alkenes, went unmeasured during the WINTER campaign. The measured suite of alkenes presented a negligible daily integrated source of OH via ozonolysis (see SI Figure S6). However, oxidation of unmeasured alkenes by Cl atoms and ozone would further enhance HO<sub>x</sub> production compared to our predictions herein, thereby reinforcing our conclusion that regional anthropogenic emissions control the wintertime radical budget. Our results therefore motivate further work to more broadly explore the types of VOC and associated Cl, OH, O<sub>3</sub>, and NO<sub>3</sub> reactivity present in polluted wintertime environments.

We find HONO is most important near urban areas close to the surface (<100-m altitude) over land, contributing <8% to the projected daily radical budget within the MBL, which was typically well mixed from the surface to ~1 km. Our measurements show some support for slower daytime production of HONO from pNO<sub>3</sub><sup>−</sup> photolysis than reported by Ye et al. (2016) and more broadly consistent with that presented in Romer et al. (2018). We thus conclude that daytime HONO production and contribution to primary radicals remain uncertain, but is likely smaller than previous estimates would have suggested.

The dominant sources of these less commonly considered radical precursors in polluted wintertime air arise largely from local and regional anthropogenic emissions, as opposed to background ozone. Incorporating these sources into a chemical transport model increased predicted PM<sub>2.5</sub> and export of NO<sub>x</sub> to the remote troposphere via PAN, where greenhouse gases such as O<sub>3</sub> and CH<sub>4</sub> are far more sensitive to its presence (Hudman et al., 2004). Other regions of the world, such as China, Europe, and northern India also experience elevated VOC concentrations from inefficient combustion and high NO<sub>x</sub> during winter which may mix with reactive chlorine, especially near coasts or chlorine emissions from coal combustion (Li et al., 2016; Lowe et al., 2015; Sarwar et al., 2014). Our findings therefore suggest important global-scale revisions to our understanding of wintertime pollution transformations, transport, and multiphase processes.



## Acknowledgments

This work was supported by the National Science Foundation AGS 1360745 and AGS-1822664 and NASA NNX15AT96G. The WINTER data are available online (<http://data.eol.ucar.edu>). The Framework of 0-D Atmospheric modeling employed in this work can be found here (<https://sites.google.com/site/wolfegm/models>).

## References

- Altshuler, A. P. (1993). Production of aldehydes as primary emissions and from secondary atmospheric reactions of alkenes and alkanes during the night and early morning hours. *Atmospheric Environment. Part A. General Topics*, 27(1), 21–32. [https://doi.org/https://doi.org/10.1016/0960-1686\(93\)90067-9](https://doi.org/https://doi.org/10.1016/0960-1686(93)90067-9)
- Anderson, L. G., Lanning, J. A., Barrell, R., Miyagishima, J., Jones, R. H., & Wolfe, P. (1996). Source and sinks of formaldehyde and acetaldehyde: An analysis of Denver's ambient concentration data. *Atmospheric Environment*, 30, 2113–2123. [https://doi.org/10.1016/1352-2310\(95\)00175-1](https://doi.org/10.1016/1352-2310(95)00175-1)
- Behnke, W., George, C., Scheer, V., & Zetzsch, C. (1997). Production and decay of ClNO<sub>2</sub> from the reaction of gaseous N<sub>2</sub>O<sub>5</sub> with NaCl solution: Bulk and aerosol experiments. *Journal of Geophysical Research*, 102(D3), 3795–3804. <https://doi.org/10.1029/96JD03057>
- Bertram, T. H., & Thornton, J. A. (2009). Toward a general parameterization of N<sub>2</sub>O<sub>5</sub> reactivity on aqueous particles: the competing effects of particle liquid water, nitrate and chloride. *Atmospheric Chemistry and Physics*, 9(21), 8351–8363. <https://doi.org/10.5194/acp-9-8351-2009>
- Brown, S. S., Neuman, J. A., Ryerson, T. B., Trainer, M., Dubé, W. P., Holloway, J. S., et al. (2006). Nocturnal odd-oxygen budget and its implications for ozone loss in the lower troposphere. *Geophysical Research Letters*, 33, L08801. <https://doi.org/10.1029/2006GL025900>
- Dentener, F. J., & Crutzen, P. J. (1993). Reaction of N<sub>2</sub>O<sub>5</sub> on tropospheric aerosols: Impact on the global distributions of NO<sub>x</sub>, O<sub>3</sub>, and OH. *Journal of Geophysical Research*, 98(D4), 7149–7163. <https://doi.org/10.1029/92JD02979>
- Edwards, P. M., Brown, S. S., Roberts, J. M., Ahmadov, R., Banta, R. M., deGouw, J. A., et al. (2014). High winter ozone pollution from carbonyl photolysis in an oil and gas basin. *Nature*, 514(7522), 351–354. <https://doi.org/10.1038/nature13767>
- Evans, M. J., & Jacob, D. J. (2005). Impact of new laboratory studies of N<sub>2</sub>O<sub>5</sub> hydrolysis on global model budgets of tropospheric nitrogen oxides, ozone, and OH. *Geophysical Research Letters*, 32, L09813. <https://doi.org/10.1029/2005GL022469>
- Febo, A., Perrino, C., & Allegrini, I. (1996). Measurement of nitrous acid in Milan, Italy, by DOAS and diffusion denuders. *Atmospheric Environment*, 30(21), 3599–3609. [https://doi.org/https://doi.org/10.1016/1352-2310\(96\)00069-6](https://doi.org/https://doi.org/10.1016/1352-2310(96)00069-6)
- Finlayson-Pitts, B. J., Ezell, M. J., & Pitts, J. N. (1989). Formation of chemically active chlorine compounds by reactions of atmospheric NaCl particles with gaseous N<sub>2</sub>O<sub>5</sub> and ClONO<sub>2</sub>. *Nature*, 337(6204), 241–244. <https://doi.org/10.1038/337241a0>
- Fortems-Cheiney, A., Chevallier, F., Pison, I., Bousquet, P., Saunio, M., Szopa, S., et al. (2012). The formaldehyde budget as seen by a global-scale multi-constraint and multi-species inversion system. *Atmospheric Chemistry and Physics*, 12(15), 6699–6721. <https://doi.org/10.5194/acp-12-6699-2012>
- Gao, M., Carmichael, G. R., Wang, Y., Ji, D., Liu, Z., & Wang, Z. (2016). Improving simulations of sulfate aerosols during winter haze over Northern China: the impacts of heterogeneous oxidation by NO<sub>2</sub>. *Frontiers of Environmental Science & Engineering*, 10(5), 1–11. <https://doi.org/10.1007/s11783-016-0878-2>
- Haskins, J. D., Jaeglé, L., Shah, V., Lee, B. H., Lopez-Hilfiker, F. D., Campuzano-Jost, P., et al. (2018). Wintertime gas-particle partitioning and speciation of inorganic chlorine in the lower troposphere over the Northeast United States and Coastal Ocean. *Journal of Geophysical Research: Atmospheres*, 123, 12,897–12,916. <https://doi.org/10.1029/2018JD028786>
- Haskins, J. D., Lee, B. H., Lopez-Hilfiker, F. D., Peng, Q., Jaeglé, L., Reeves, J. M., et al. (2019). Observational constraints on the formation of Cl<sub>2</sub> from the reactive uptake of ClNO<sub>2</sub> on aerosols in the polluted marine boundary layer. *Journal of Geophysical Research: Atmospheres*, 124, 8851–8869. <https://doi.org/10.1029/2019JD030627>
- Heald, C. L., Collett, J. L. Jr., Lee, T., Benedict, K. B., Schwandner, F. M., Li, Y., et al. (2012). Atmospheric ammonia and particulate inorganic nitrogen over the United States. *Atmospheric Chemistry and Physics*, 12, 10,295–10,312. <https://doi.org/10.5194/acp-12-10295-2012>
- Hudman, R. C., Jacob, D. J., Cooper, O. R., Evans, M. J., Heald, C. L., Park, R. J., et al. (2004). Ozone production in transpacific Asian pollution plumes and implications for ozone air quality in California. *Journal of Geophysical Research*, 109, D23S10. <https://doi.org/10.1029/2004JD004974>
- Jaeglé, L., Shah, V., Thornton, J. A., Lopez-Hilfiker, F. D., Lee, B. H., McDuffie, E. E., et al. (2018). Nitrogen oxides emissions, chemistry, deposition, and export over the northeast United States during the WINTER aircraft campaign. *Journal of Geophysical Research: Atmospheres*, 123, 12,368–12,393. <https://doi.org/10.1029/2018JD029133>
- Kelly, T. J., Smith, D. L., & Satola, J. (1999). Emission rates of formaldehyde from materials and consumer products found in California Homes. *Environmental Science & Technology*, 33(1), 81–88. <https://doi.org/10.1021/es980592>
- Kirchstetter, T. W., Harley, R. A., & Littlejohn, D. (1996). Measurement of nitrous acid in motor vehicle exhaust. *Environmental Science & Technology*, 30(9), 2843–2849. <https://doi.org/10.1021/es960135y>
- Kleffmann, J. (2007). Daytime sources of nitrous acid (HONO) in the atmospheric boundary layer. *ChemPhysChem*, 8(8), 1137–1144. <https://doi.org/10.1002/cphc.200700016>
- Levy, H. (1971). Normal atmosphere: Large radical and formaldehyde concentrations predicted. *Science*, 173(3992), 141–143. <https://doi.org/10.1126/science.173.3992.141>
- Li, Q., Zhang, L., Wang, T., Tham, Y. J., Ahmadov, R., Xue, L., et al. (2016). Impacts of heterogeneous uptake of dinitrogen pentoxide and chlorine activation on ozone and reactive nitrogen partitioning: Improvement and application of the WRF-Chem model in southern China. *Atmospheric Chemistry and Physics*, 16(23), 14875–14,890. <https://doi.org/10.5194/acp-16-14875-2016>
- Lowe, D., Archer-Nicholls, S., Morgan, W., Allan, J., Utembe, S., Ouyang, B., et al. (2015). WRF-Chem model predictions of the regional impacts of N<sub>2</sub>O<sub>5</sub> heterogeneous processes on night-time chemistry over north-western Europe. *Atmospheric Chemistry and Physics*, 15(3), 1385–1409. <https://doi.org/10.5194/acp-15-1385-2015>
- Luecken, D. J., Hutzell, W. T., Strum, M. L., & Pouliot, G. A. (2012). Regional sources of atmospheric formaldehyde and acetaldehyde, and implications for atmospheric modeling. *Atmospheric Environment*, 47, 477–490. <https://doi.org/https://doi.org/10.1016/j.atmosenv.2011.10.005>
- McDonald, B. C., de Gouw, J. A., Gilman, J. B., Jathar, S. H., Akherati, A., Cappa, C. D., et al. (2018). Volatile chemical products emerging as largest petrochemical source of urban organic emissions. *Science*, 359(6377), 760–764. <https://doi.org/10.1126/science.aaq0524>
- McDuffie, E. E., Fibiger, D. L., Dubé, W. P., Lopez Hilfiker, F., Lee, B. H., Jaeglé, L., et al. (2018). ClNO<sub>2</sub> yields from aircraft measurements during the 2015 WINTER campaign and critical evaluation of the current parameterization. *Journal of Geophysical Research: Atmospheres*, 123, 913–994. <https://doi.org/10.1029/2018JD029358>
- McDuffie, E. E., Fibiger, D. L., Dubé, W. P., Lopez-Hilfiker, F., Lee, B. H., Thornton, J. A., et al. (2018). Heterogeneous N<sub>2</sub>O<sub>5</sub> uptake during winter: Aircraft measurements during the 2015 WINTER campaign and critical evaluation of current parameterizations. *Journal of Geophysical Research: Atmospheres*, 123, 4345–4372. <https://doi.org/10.1002/2018JD028336>
- Michoud, V., Kukui, A., Camredon, M., Colomb, A., Borbon, A., Miet, K., et al. (2012). Radical budget analysis in a suburban European site during the MEGAPOLI summer field campaign. *Atmospheric Chemistry and Physics*, 12, 11,951–11,974. <https://doi.org/10.5194/acp-12-11951-2012>



- Orlando, J. J., Tyndall, G. S., Apel, E. C., Riemer, D. D., & Paulson, S. E. (2003). Rate coefficients and mechanisms of the reaction of Cl-atoms with a series of unsaturated hydrocarbons under atmospheric conditions. *International Journal of Chemical Kinetics*, 35(8), 334–353. <https://doi.org/10.1002/kin.10135>
- Platt, U. F., Winer, A. M., Biermann, H. W., Atkinson, R., & Pitts, J. N. (1984). Measurement of nitrate radical concentrations in continental air. *Environmental Science & Technology*, 18(5), 365–369. <https://doi.org/10.1021/es00123a015>
- Riedel, T. P., Wolfe, G. M., Danas, K. T., Gilman, J. B., Kuster, W. C., Bon, D. M., et al. (2014). An MCM modeling study of nitryl chloride (ClNO<sub>2</sub>) impacts on oxidation, ozone production and nitrogen oxide partitioning in polluted continental outflow. *Atmospheric Chemistry and Physics*, 14(8), 3789–3800. <https://doi.org/10.5194/acp-14-3789-2014>
- Riemer, N., Vogel, H., Vogel, B., Schell, B., Ackermann, I., Kessler, C., & Hass, H. (2003). Impact of the heterogeneous hydrolysis of N<sub>2</sub>O<sub>5</sub> on chemistry and nitrate aerosol formation in the lower troposphere under photochemical conditions. *Journal of Geophysical Research: Atmospheres*, 108(D4). <https://doi.org/10.1029/2002JD002436>
- Romer, P. S., Wooldridge, P. J., Crouse, J. D., Kim, M. J., Wennberg, P. O., Dibb, J. E., et al. (2018). Constraints on aerosol nitrate photolysis as a potential source of HONO and NO<sub>x</sub>. *Environmental Science & Technology*, 52(23), 13,738–13,746.
- Sarwar, G., Simon, H., Xing, J., & Mathur, R. (2014). Importance of tropospheric ClNO<sub>2</sub> chemistry across the Northern Hemisphere. *Geophysical Research Letters*, 41, 4050–4058. <https://doi.org/10.1002/2014GL059962>
- Schroder, J. C., Campuzano-Jost, P., Day, D. A., Shah, V., Larson, K., Sommers, J. M., et al. (2018). Sources and secondary production of organic aerosols in the northeastern United States during WINTER. *Journal of Geophysical Research: Atmospheres*, 123, 7771–7796. <https://doi.org/10.1029/2018JD028475>
- Shah, V., Jaeglé, L., Thornton, J. A., Lopez-Hilfiker, F. D., Lee, B. H., Schroder, J. C., et al. (2018). Chemical feedbacks weaken the wintertime response of particulate sulfate and nitrate to emissions reductions over the eastern United States. *Proceedings of the National Academy of Sciences*, 115(32), 8110–8115. <https://doi.org/10.1073/pnas.1803295115>
- Sigsby, J. E., Tejada, S., Ray, W., Lang, J. M., & Duncan, J. W. (1987). Volatile organic compound emissions from 46 in-use passenger cars. *Environmental Science & Technology*, 21(5), 466–475. <https://doi.org/10.1021/es00159a007>
- Sorgel, M., Regelin, E., Bozem, H., Diesch, J. M., Drewnick, F., Fischer, H., et al. (2011). Quantification of the unknown HONO daytime source and its relation to NO<sub>2</sub>. *Atmospheric Chemistry and Physics*, 11(20), 10,433–10,447. <https://doi.org/10.5194/acp-11-10433-2011>
- Spataro, F., & Ianniello, A. (2014). Sources of atmospheric nitrous acid: State of the science, current research needs, and future prospects. *Journal of the Air & Waste Management Association*, 64(11), 1232–1250. <https://doi.org/10.1080/10962247.2014.952846>
- Stutz, J., Alicke, B., & Neftel, A. (2002). Nitrous acid formation in the urban atmosphere: Gradient measurements of NO<sub>2</sub> and HONO over grass in Milan, Italy. *Journal of Geophysical Research*, 107(D22), 8192. <https://doi.org/10.1029/2001JD000390>
- Sullivan, A. P., Guo, H., Schroder, J. C., Campuzano-Jost, P., Jimenez, J. L., Campos, T., et al. (2019). Biomass burning markers and residential burning in the WINTER aircraft campaign. *Journal of Geophysical Research: Atmospheres*, 124, 1846–1861. <https://doi.org/10.1029/2017JD028153>
- Tesche, T. W., Morris, R., Tonnesen, G., McNally, D., Boylan, J., & Brewer, P. (2006). CMAQ/CAMx annual 2002 performance evaluation over the eastern US. *Atmospheric Environment*, 40(26), 4906–4919. <https://doi.org/https://doi.org/10.1016/j.atmosenv.2005.08.046>
- VandenBoer, T. C., Murphy, J. G., Roberts, J. M., Middlebrook, A. M., Brock, C. A., Lerner, B., et al. (2013). Understanding the role of the ground surface in HONO vertical structure: High resolution vertical profiles during NACHTT-11. *Journal of Geophysical Research: Atmospheres*, 118, 10,155–10,171. <https://doi.org/10.1002/jgrd.50721>
- Volkamer, R., Sheehy, P., Molina, L. T., & Molina, M. J. (2010). Oxidative capacity of the Mexico City atmosphere—Part I: A radical source perspective. *Atmospheric Chemistry and Physics*, 10, 6969–6991. <https://doi.org/10.5194/acp-10-6969-2010>
- Walker, J. M., Philip, S., Martin, R. V., & Seinfeld, J. H. (2012). Simulation of nitrate, sulfate, and ammonium aerosols over the United States. *Atmospheric Chemistry and Physics*, 12(22), 11,213–11,227. <https://doi.org/10.5194/acp-12-11213-2012>
- Whalley, L. K., Stone, D., Dunmore, R., Hamilton, J., Hopkins, J. R., Lee, J. D., et al. (2018). Understanding in situ ozone production in the summertime through radical observations and modelling studies during the Clean air for London project (ClearLo). *Atmospheric Chemistry and Physics*, 18, 2547–2571. <https://doi.org/10.5194/acp-18-2547-2018>
- Wolfe, G. M., Kaiser, J., Hanisco, T. F., Keutsch, F. N., de Gouw, J. A., Gilman, J. B., et al. (2016). Formaldehyde production from isoprene oxidation across NO<sub>x</sub> regimes. *Atmospheric Chemistry and Physics*, 16(4), 2597–2610. <https://doi.org/10.5194/acp-16-2597-2016>
- Wolfe, G. M., Marvin, M. R., Roberts, S. J., Travis, K. R., & Liao, J. (2016). The Framework for 0-D Atmospheric Modeling (F0AM) v3.1. *Geoscientific Model Development*, 9(9), 3309–3319. <https://doi.org/10.5194/gmd-9-3309-2016>
- Wong, K. W., Tsai, C., Lefter, B., Haman, C., Grossberg, N., Brune, W. H., et al. (2012). Daytime HONO vertical gradients during SHARP 2009 in Houston, TX. *Atmospheric Chemistry and Physics*, 12(2), 635–652. <https://doi.org/10.5194/acp-12-635-2012>
- Ye, C., Zhou, X., Pu, D., Stutz, J., Festa, J., Spolaor, M., et al. (2016). Rapid cycling of reactive nitrogen in the marine boundary layer. *Nature*, 532(7600), 489. Retrieved from—491. <https://doi.org/10.1038/nature17195>
- Yienger, J. J., Klonecki, A. A., Levy, H., Moxim, W. J., & Carmichael, G. R. (1999). An evaluation of chemistry's role in the winter-spring ozone maximum found in the northern midlatitude free troposphere. *Journal of Geophysical Research*, 104(D3), 3655–3667. <https://doi.org/10.1029/1998JD100043>
- Young, C. J., Washenfelder, R. A., Edwards, P. M., Parrish, D. D., Gilman, J. B., Kuster, W. C., et al. (2014). Chlorine as a primary radical: Evaluation of methods to understand its role in initiation of oxidative cycles. *Atmospheric Chemistry and Physics*, 14, 3427–3440. <https://doi.org/10.5194/acp-14-3427-2014>